JVI Accepted Manuscript Posted Online 14 September 2016
J. Virol. doi:10.1128/JVI.01532-16

HIV envelope gp120 alters T-cell receptor mobilization in the immunological synapse of uninfected CD4 T cells and augments the T cell activation

Jing Deng[1,2], Yu-ya Mitsuki[3], Guomiao Shen[2], Jocelyn Ray[4], Claudia Cicala[4], James Arthos[4], Michael L. Dustin[1,5], Catarina E. Hioe[3,6#]

[1]Skirball Institute of Biomolecular Medicine, New York University School of Medicine, New York, New York, United States of America

[2]Department of Pathology, New York University School of Medicine, New York, New York, United States of America

[3]Icahn School of Medicine at Mount Sinai, Division of Infectious Diseases, New York, New York, United States of America

[4]Laboratory of Immunoregulation, National Institute of Allergy and Infectious Diseases, National Institutes of Health, Bethesda, Maryland, United States of America

[5]The Kennedy Institute of Rheumatology, Nuffield Department of Orthopaedics and Musculoskeletal Sciences, The University of Oxford, Headington, United Kingdom

[6]James J. Peters Veterans Affairs Medical Center, Research Service, Bronx, New York, United States of America

Short title: CD4 T-cell Activation by HIV Env at Immune Synapse

[#]Corresponding author.

Email: catarina.hioe@mssm.edu (CEH)

Abstract

HIV is transmitted most efficiently from cell to cell and productive infection occurs mainly in activated CD4 T cells. It is postulated that HIV exploits immunological synapses formed between CD4 T cells and antigen-presenting cells to facilitate the targeting and infection of activated CD4 T cells. This study sought to evaluate how the presence of the HIV envelope (Env) in the CD4 T cell immunological synapse affects synapse formation and intracellular signaling to impact the downstream T cell activation events. CD4 T cells were applied onto supported lipid bilayers (SLBs) that were reconstituted with HIV Env gp120, anti-TCR antibody OKT3 and ICAM-1 to represent the surface of HIV Env-bearing antigen-presenting cells. The results showed that the HIV Env did not disrupt immunological synapse formation. Instead, the HIV Env accumulated with TCR at the center of the synapse, altered the kinetics of TCR recruitment to the synapse, and affected the synapse morphology over time. The HIV Env also prolonged Lck phosphorylation at the synapse and enhanced TCR-induced CD69 upregulation, IL-2 secretion, and proliferation to promote virus infection. These results suggest that HIV uses the immunological synapse as a conduit not only for selective virus transmission to activated CD4 T cells, but also for boosting the T cell activation state, thereby increasing its likelihood for undergoing productive replication in the targeted CD4 T cells.

Importance

There are about two million new HIV infections every year. A better understanding on how HIV is transmitted to the susceptible cells is critical to devise effective strategies to prevent HIV infection. Activated CD4 T cells are preferentially infected by HIV, although how this is accomplished is not fully understood. This study examined whether HIV co-

Journal of Virology JVI Journal of Virology

opts the normal T-cell activation process through the so-called immunological synapse. We found that the HIV envelope is recruited to the center of the immunological synapse together with the T-cell receptor and enhances the T cell receptor-induced activation of the CD4 T cells. The heightened cellular activation promotes the capacity of the CD4 T cells to support productive HIV replication. This study provides evidence for the exploitation of the normal immunological synapse and T-cell activation process by HIV to boost the activation state of the targeted CD4 T cells and promote infection of these cells.

Introduction

HIV infection leads to severe destruction of immune cells and functions. The helper CD4 T cells are one of the main cell types profoundly affected by HIV (1, 2). However, not all CD4 T cells are equally affected by HIV. Although HIV can infect resting naïve CD4 T cells, these cells predominantly express the co-receptor CXCR4 and are less likely to express the co-receptor CCR5 required for the entry of the majority of transmitted and circulating HIV-1 isolates. In contrast, many memory CD4 T cells express the co-receptors CXCR4 and CCR5 (3, 4). The post-entry steps in the HIV life cycle are also tightly linked to the activation status of the CD4 T cells. Reverse transcription (5, 6), nuclear import (7), and integration (8) are inefficient unless the CD4 T cells are activated and enter the cell cycle. Virus transcription is triggered via NFκB (9), which is activated as a result of the specific signaling cascade triggered upon TCR engagement. Therefore, TCR-activated CD4 T cells are the optimal targets for HIV. Indeed, the recruitment of activated CD4 T cells to the genital or rectal mucosa associated with HSV-2, gonorrhea, and other STDs is considered to be one of the factors that increase the risk for HIV acquisition (10-12). Studies of SIV and SHIV infections in rhesus macaques also showed that the increased numbers of activated CD4 T cells at the site of virus entry constitutes one of the correlates for the increased infection (13, 14). However, the mechanisms by which HIV preferentially targets the activated subsets of CD4 T cells are not fully understood.

CD4 T cell activation commences in an immunological synapse, a tight junction at the contact site between a CD4 T cell and an antigen-presenting cell (APC) formed

when the CD4 T cell recognizes the cognate peptide-MHC class II (pMHC) complexes on the APC (reviewed in (15, 16)). A CD4 T cell will stop migrating once it has formed an immunological synapse (17). At the periphery of the synaptic area, pMHC/TCR interactions form microclusters which quickly translocate to the center and converge to become the central supramolecular activation cluster (cSMAC) (18, 19). At the same time, ICAM-1/LFA-1 interactions begin clustering to form the peripheral SMAC (pSMAC). A mature stable synapse is thus created with a fully segregated cSMAC and pSMAC ring which arrests the cell migration for over one hour. Recent correlative optical/electron microscopy analyses of the immunological synapse formed on surrogate antigen-presenting cells based on lipid bilayers have provided higher resolution pictures showing the cSMAC region as a cleft containing TCR-rich vesicles (20). These images are highly reminiscent of the electron tomographic data showing the accumulation of HIV virions in the contact area formed between a primary CD4 T cell target and an infected T cell (21).

The cell-cell contact area implicated in facilitating the highly efficient HIV transmission from one cell to another is called the virological synapse (22-26). This synapse has similar morphology and utilize many components of the immunological synapse, although the two types of synapses also display distinctive features (27). The assembly of virological synapses is triggered by the binding of the HIV Env on infected cells to CD4 on the target cells and can occur independently of TCR-pMHC engagement (28). Similar to the immunological synapse, the formation of the HIV Env-induced synapse also results in the arrest of CD4 T cell migration (28). During this time, HIV Env-CD4 microclusters form and quickly converge to assemble a cSMAC-like

cluster surrounded by the pSMAC-like ICAM-1/LFA-1 ring (29). The TCR alpha beta chains are also recruited to the cSMAC-like cluster albeit in the absence of cognate pMHCs (29). However, when CD4 T cells encounter HIV-infected APCs, simultaneous HIV Env-CD4 and TCR-pMHC engagements ensue and the consequences of such interactions remain unclear.

As a result of TCR-pMHC engagement at the immunological synapse, T cells receive a series of activation signals (reviewed in (15)). The TCR activation signals begin with the rapid recruitment and activation of Src kinases, Lck and Fyn (18, 19, 30). The signals propagate downstream leading to the phosphorylation of phospholipase C-γ1 (PLC-γ1) and the hydrolysis of phosphatidylinositol 4,5-bisphosphate (PIP2). This results in the production of the second messengers diacylglycerol (DAG) and inositol trisphosphate (IP3), the activation of transcription factor NFκB via PKCθ and the MAPK/Erk pathways, the flux of intracellular Ca^{2+}, and the transcription of IL-2 via Ca^{2+}-associated calmodulin, calcineurin and NFAT. Of note, the TCR-induced signaling cascade is transient; it is initiated at the newly formed TCR-pMHC microclusters and terminated at the cSMAC (18, 30). CD4 distribution is consistent with these data in that CD4 initially associates with the TCR-pMHC microclusters yet does not accumulate in the cSMAC (31). The lack of active signaling at the cSMAC is also explained by the finding that TCRs associated with micro-vesicles are detached and released out of the cell into the synaptic cavity from the cSMAC (20).

A similar but atypical signaling cascade is triggered in the HIV Env-induced virological synapse (29). The HIV Env-CD4 interactions at the synapse lead to the phosphorylation of Lck and the downstream TCR signalosome components CD3ζ, ZAP-

70, LAT, SLP-76, Itk, and PLC-γ1 (29). These signaling molecules accumulate in the cSMAC-like central Env/CD4 cluster and retain their phosphorylation for more than one hour, even after the synapse breaks and the cell resumes migration. Notably, the protracted signaling does not lead to full T-cell activation as indicated by lack of PKCθ activation and no elevation of Ca^{2+} or CD69. Nonetheless, the Env-induced signals trigger actin polymerization to create an F-actin ring with a depleted central zone implicated to serve as a channel for efficient transport of the HIV virions within the target CD4 T cell (29). These signals also activate LFA-1 on naïve CD4 T cells (32).

In this study, we postulate that the aberrant HIV Env-triggered signaling exerts a dominant effect on the TCR-induced activation signals at the immunological synapse to impact the activation state of CD4 T cells targeted by the virus. We utilized a supported lipid bilayer (SLB) system that has been used to monitor the immunological synapses formed by CD4 T cells, CD8 T cells, and NK cells and the signaling molecules recruited to the various synapses (18, 19, 28, 29, 33, 34). To evaluate the specific contribution of the HIV Env in the CD4 T cell immunological synapse, we applied primary activated CD4 T cells onto SLB constituted with OKT3 (an anti-CD3 monoclonal antibody that engages TCR), ICAM-1 (a key adhesion molecule integral to the immunological synapse), and plus or minus HIV Env gp120. Although the HIV Env did not disrupt the immunological synapse formation, its presence at the synapse affected the kinetics of TCR mobilization and the synapse morphology. Further, the HIV Env induced temporal and spatial alterations to the most proximal TCR-associated signaling molecule Lck and augmented CD4 T cell activation and proliferation. These data support the notion that HIV co-opts the immunological synapse to disseminate to highly vulnerable CD4 T cells

142 undergoing TCR-induced activation and promote its replication by heightening the T cell
143 activation state.

144 **Materials and Methods**

145 **Cells.** Peripheral blood mononuclear cells were isolated from leukopacks of
146 anonymous healthy donors (purchased from New York Blood Center) using Ficoll-
147 Hypaque. Approval for the use of human specimens was obtained from the New York
148 University School of Medicine Institutional Research Board. CD4 T cells or CD8 T cells
149 were enriched by using CD4 or CD8 negative-selection magnetic bead kits (STEMCELL
150 Technologies). The T cells were then activated on plates coated with anti-CD3 and anti-
151 CD28 antibodies at 5 μg/ml each. After 48 h, activated cells were transferred onto new
152 plates at a density of 1×10^6 cells/ml and supplemented with 20U/ml interleukin-2. Cells
153 were used in the SLB experiments 5 to 12 days later.
154

155 **Supported lipid bilayers (SLBs).** SLBs were prepared as described (35) with
156 some modifications. Liposomes containing DOPC (Avanti Polar Lipids) supplemented
157 with 12.5 % 1,2-dioleoylsn-glycero-3-[(N-(5-amino-1-carboxypentyl)iminodiacetic acid)-
158 succinyl] nickel salt (Ni-NTA-DOGS) and 0.005% 1,2-dipalmitoyl-sn-glycero-3-
159 phosphoethanolamine-N-(Cap biotinyl) were applied onto clean coverslips placed onto
160 sticky-Slide VI 0.4 chambers (Ibidi). After blocking with 5% casein containing 100 μM
161 $NiCl_2$, His_{12}-tagged HIV gp120 SF162 (250/μm^2) and ICAM-1 (200/μm^2) were added to
162 bind Ni-NTA-DOGS, while mono-biotinylated OKT3 (30/μm^2) was attached to Cap-
163 biotinyl. All proteins were also fluorescently labelled prior to addition to the SLBs. The
164 density of HIV gp120 tested on the SLBs was established in our previous studies (28).
165 For comparison, the estimated Env density on the surface of HIV virions is 8 to 14
166 envelope spikes per virion (36, 37), which correspond to 250 to 450/μm^2 for virions with

a diameter of ~100 nm. On the cell surface, the HIV envelope glycoproteins are expressed in patches (38, 39), and the confocal microscopy measurements of the local densities of HIV gp120 at such patches on the HIV envelope-transfected cell surfaces yielded an average density of 369 molecules/μm^2 (median, 287 molecules/μm^2; range, 0-2490 molecules/μm^2) ((28) and data not shown). The ICAM-1 and OKT3 densities of on the SLB were based on their expression levels on the surfaces of antigen-presenting cells (28). The density of each protein was determined prior to use in the SLBs by coating the same SLB preparations onto 5-μm-diameter silica beads and analyzing the beads by flow cytometry using calibration beads (Bangs Laboratories Inc., IN). The SLBs were then washed, and incubated with 0.5×10^6 cells in 200 μl HEPES-buffered saline containing 1% human serum albumin, 2 mM $MgCl_2$, and 1 mM $CaCl_2$.

Immunofluorescence staining was used to detect total and phosphorylated Lck at the immunological synapse. At the designated time points, cells on SLBs were fixed with 2% paraformaldehyde, permeabilized with 0.1% Triton X-100, and stained with antibodies specific for Lck phosphorylated on Y394 (R&D Systems) or Y505 (BD Transduction Laboratories) or total Lck (BD™ Phosflow), followed with an appropriate Alexa Fluor 546-labeled secondary antibody (Invitrogen,CA).

For antibody-blocking experiments, anti-gp120 mAbs obtained from Drs. Susan Zolla-Pazner (Icahn School of Medicine at Mount Sinai) and Miroslaw K. Gorny (NYU School of Medicine) were used (40-42). SLBs containing OKT3, ICAM-1 and gp120 were treated with 10 μg/ml of mAb for 30 minutes prior to introduction of the cells and washed three times with the assay buffer to remove excess mAb. The mAbs 654, 2158, and 2558 have potent neutralizing activities against HIV-1 SF162 from which the gp120

protein used in this study was derived (IC_{50} titers of <1, 6, <1 μg/ml, respectively (43)). The control mAb 1418 is specific for parvovirus and does not neutralize HIV.

Total Internal Reflection Fluorescence Microscopy. T cells were loaded onto SLBs and allowed to interact for approximately 1 hour or for the indicated times. Images were acquired either from live cells or after fixation and staining. Fluorescence microscopy and IRM were performed on a Nikon Ti microscope with a TIRF module and an Andor DU897 back illuminated electron multiplier EMCCD camera. Solid-state lasers provided illumination at 405, 488, 561, and 641 nm and narrow pass filters were used for detection.

Image analysis. Acquisition settings were maintained constant throughout each imaging procedure and between samples. Image analysis was performed with ImageJ. To measure intensities, individual-cell contacts were traced with region of interest (ROI) on the IRM channel. Images were subtracted for background, and then cells in the subtracted images were marked with ROIs.

The densities of gp120 were calculated by measuring the fluorescence intensity values from gp120-AF488 channel within each cell and subtracting them with the background values from SLBs with no gp120. The gp120 densities on the OKT3+ICAM-1+gp120 SLBs in the areas with no cell contacts were normalized to 250 molecules/μm^2. The densities of OKT3 were measured based on the fluorescence intensity values from the OKT3-AF647 channel minus the background values. The OKT3 background values were calculated from the zero time-point and normalized to 30

213 molecules/μm^2.

214 Measurement of signaling molecules in cells on the SLBs was done on the entire
215 cell-SLB contact area as detected in the IRM channel (29). Average fluorescence
216 intensity was measured in each of the areas designated above. The background
217 fluorescence was subtracted from the average intensity. The integrated fluorescence
218 intensity was then calculated by multiplying the average intensity by the total pixel area
219 measured in each cell. The pixel area was converted to μm^2 based on the pixel/μm^2
220 ratio for the specific cameras and objectives that were used.

221

222 **CD69 upregulation and IL-2 secretion.** CD4 T cells were activated with anti-
223 CD3 and anti-28 mAbs as described above and used at least 7 days post-activation.
224 CD4 T cells (0.5×10^6 per condition) were incubated with silica beads of 5 μm in
225 diameter (Bangs Laboratories), the standard bead size for T cell stimulation and
226 expansion (44). The beads were coated with SLBs containing OKT3, ICAM-1, plus or
227 minus CD80 or HIV gp120. After 6 hours, cells were stained with anti-human CD69 PE
228 Abs (eBioscience) and analyzed by FACSCalibur (BD). At 24 hours, supernatants were
229 collected and IL-2 concentrations were measured by using human IL-2 ELISA Kit
230 (Thermo scientific).

231

232 **T cell proliferation and HIV replication**. To measure proliferation, CD4 T cells
233 freshly isolated from peripheral blood were labeled with CSFE, cultured on wells coated
234 with OKT3 plus or minus HIV gp120. Anti-CD4 mAb Leu3A was also tested to block
235 CD4 interaction with HIV gp120. After 5 days, cell proliferation was measured based on

CFSE dilution by flow cytometry, and the data were analyzed with FlowJo. These stimulated CD4 T cells were also assessed for the ability to support virus replication. After culture with OKT3, OKT3+HIV gp120, or OKT3+anti-CD28 mAb for 5 days, the cells were infected with HIV-1 SF162 (moi=0.1 as measured in the MT4-TMZ-R5 reporter cells), washed and incubated in the presence of the same stimuli for an additional 10 days, without the addition of exogenous cytokines. Virus production was monitored in the supernatants at day 3 and day 10 post-infection by p24 ELISA (XpressBio).

Statistics. The graphs and statistical analyses were performed with Microsoft Excel and Graphpad Prism. Experiments were performed at least three times.

Results

CD4 T cell immunological synapse formation and TCR recruitment to the synapse in the presence of HIV Env gp120

In order to study the effect of the HIV Env on the formation of TCR-induced immunological synapse in primary human CD4 T cells, we used the SLB as an experimental model. This system enables the real-time visualization of microclusters and supramolecular activation clusters (SMAC) as they form in the TCR-induced immunological synapse and in the TCR-independent HIV Env gp120-induced virological synapse (18, 19, 28, 29). The SLBs were constituted with the anti-CD3 mAb OKT3, ICAM-1 and HIV Env gp120 to represent the surface of APCs expressing HIV Env following infection. A recombinant monomeric HIV-1 (SF162) gp120 with a His_{12} tag at its C terminus was labeled with the fluorescent dye Alexa Fluor 488 (AF488-gp120) and attached to the SLB via Ni^{2+}-chelating NTA lipids. ICAM-1 was also tagged with His_{12} but was labeled with Alexa Fluor 405. Anti-CD3 mAb OKT3 was mono-biotinylated, labeled with Alexa Fluor 647, and reacted sequentially with streptavidin and the biotin-CAP present in the SLBs. Activated CD4 T cells were then added onto the SLBs and live images were acquired by total internal reflection fluorescence microscopy (TIRFM) for 1 hour (**Fig 1**). The previously activated CD4 T cells were used to allow the evaluation of a relatively homogenous population of primary target cells that are permissive to HIV infection and form well-defined immunological synapses on SLBs (18, 19, 28, 29).

Within 10 minutes after the CD4 T cells had interacted with OKT3 and ICAM-1 on the SLBs, typical immunological synapses displaying the TCR-rich cSMAC and the

ICAM-1 pSMAC rings were assembled in the absence of the HIV Env (**Fig 1A, top panel**). In the presence of HIV gp120 on the SLBs, the cells also formed synapses with segregated cSMAC and pSMAC (**Fig 1A, bottom panel**). These synapses were similar to those formed on SLBs without gp120. Notably, HIV gp120 accumulated in the center of the synapse and coalesced together with TCR at the cSMAC (**Fig 1A**). The relative distribution of HIV gp120 and TCR in the synapse was quantified by determining the densities of gp120 and OKT3 along the cell radius. Data were acquired at the 10-minute time point from a minimum of 30 cells per condition. These data confirmed the visual observation in **Fig 1A** and demonstrated an increase of gp120 density from an initial density of 250 molecules/μm^2 on the SLBs to 400 molecules/μm^2 at the center of the cell (**Fig 1B left**). Measurements also showed an increase in OKT3 density towards the center of the synapse and an accumulation of OKT3 at the cSMAC that was ~3x fold higher ($p < 0.0001$) in the presence of HIV gp120 (**Fig 1B right**), indicating that HIV gp120 may help augment TCR recruitment and clustering at the cSMAC.

For comparison, we also evaluated the effect of HIV gp120 on the immunological synapse formed by CD8 T cells. Activated CD8 T cells were applied to the SLBs containing OKT3, ICAM-1 and plus or minus gp120. The CD8 T cells formed immunological synapses with the typical bull's eye appearance comprising of the TCR-rich cSMAC and the ICAM-1 pSMAC ring on the SLBs with or without gp120 (**Fig 1C upper panel and lower panel**). However, little gp120 was recruited to the centers of the immunological synapses formed by the CD8 T cells (**Fig 1C lower panel and Fig 1D left**). The OKT3 accumulation at the c-SMAC was also not significantly increased (**Fig 1D right**). These results indicate that HIV gp120 binds primarily to CD4 T cells and

augments TCR accumulation in the CD4 T cell immunological synapse.

To further examine the alteration of TCR recruitment by HIV gp120, we compared the kinetics of OKT3 signal accumulation in the synapse over time in the presence versus the absence of gp120. CD4 T cells were introduced to the SLBs bearing OKT3, ICAM-1, and gp120 or with the SLBs with only OKT3 and ICAM-1, and the OKT3 signals were measured for 50 minutes. In the absence of gp120, OKT3 signals increased to a plateau of approximately 60-70 molecules/μm^2 at 7 minutes (**Fig 2A-B** (also see **Movie S1** for video images). This plateau was then maintained for up to 50 minutes. In contrast, when HIV gp120 was present, OKT3 signals increased more dramatically, peaking at 150 molecules/μm^2 at 7 minutes, but subsequently declined over time (**Fig 2A-B and Movie S2**).

On the SLBs with OKT3, ICAM-1 and gp120, the kinetics of gp120 accumulation was also evaluated. The HIV gp120 density increased to 400 molecules/μm^2 in approximately 10 minutes and continued to rise at a lower rate (**Fig 2C and Movie S2**). The gp120 signals fluctuated during the 50-minute observation time, but they did not show a steady decline as seen with OKT3. In fact, from 20 to 50 minutes the gp120 signals became more prominent than the OKT3 signals. Hence, the pattern of TCR accumulation did not follow that of gp120. Taken together with the data in **Fig 1**, these data demonstrate that the presence of HIV gp120 in the CD4 T cell immunological synapse HIV gp120 does not prevent the synapse formation. However, the HIV gp120 is recruited to the cSMAC along with TCR, albeit with distinct patterns, and causes a dramatic change in the kinetics of TCR recruitment and retention in the synapse.

Effects of anti-gp120 antibodies on the recruitment of HIV gp120 and TCR to the synapse

To determine the interactions involved in HIV gp120 recruitment to the CD4 T-cell immunological synapse, we pre-treated SLBs containing gp120, OKT3 and ICAM-1 with human mAbs directed to different regions of gp120. The CD4 T cells were then added and allowed to interact with the SLBs. After 20 minutes, cells were fixed and HIV gp120 densities in the synapses were measured. The results showed that mAbs against the CD4-binding site (654), the V1V2 domain (2158) and the V3 loops (2558) significantly reduced the densities of HIV gp120 at the synapses, while the irrelevant mAb control (1418) did not have this effect (**Fig 3A**). Representative images of the individual cells further showed that the anti-gp120 mAb treatment decreased the amounts of HIV gp120 at the synapses but did not block clustering (**Fig 3C**). The location of the HIV gp120 clusters near the TCR-rich cSMAC also remained unchanged. Notably, low levels of gp120 interactions remained after treatment with the mAbs, including mAb 654 that blocks CD4-gp120 binding. These findings are similar to our past study in which the mAb against the CD4-binding site also did not completely abrogate the CD4 T cell interactions with HIV gp120 on the SLBs presenting only gp120 and ICAM-1 (28). The data indicate that, in addition to CD4, other receptors are also engaged by HIV gp120 at these synapses and these interactions cannot be completely blocked by a single anti-gp120 mAb. Nonetheless, the non-CD4 receptors and their relative contributions are yet to be delineated.

Measurements of OKT3 density showed higher levels of OKT3 at the synapses in the presence of HIV gp120 (**Fig 3B**), which is consistent with data in **Fig 1 and 2.**

Pre-treatment with the anti-gp120 mAbs did not significantly affect the enhanced OKT3 accumulation. The OKT3 densities were slightly reduced by mAbs against the CD4-binding site (654) and the V3 loop (2558), but the decrease did not reach statistical significance. Hence, mAbs directed to the different sites of gp120 reduced HIV gp120 recruitment to the synapse without significantly curtailing the TCR accumulation. These data suggest that the presence of very low amounts of HIV gp120 in the synapse is sufficient for the increased OKT3 recruitment.

Effects of HIV gp120 on the synapse morphology over time

The ability of HIV gp120 to alter the kinetics of TCR accumulation and retention in the synapse suggests that HIV gp120 may affect the synapse morphology over time. To evaluate this idea, we monitored the synapses 10 and 30 minutes after CD4 T cells made contact with SLBs presenting HIV gp120, OKT3, and ICAM-1 as compared to the synapses on control SLBs containing only OKT3 and ICAM-1. On the control SLBs, 70% of the CD4 T cells formed the so-called mature immunological synapses within 10 minutes. These cells form stable contacts with the SLBs and the synapses displayed the hallmark central OKT3 cluster (cSMAC) in the center surrounded by a symmetrical peripheral ICAM-1 ring (pSMAC) (**Fig 4A, OKT3+ICAM-1: symmetrical**). The ICAM-1 ring keeps the migratory T cells from crawling across the SLBs (17, 28). These synapses were maintained throughout the observation period; after 30 minutes the percentage of the cells with mature synapses remained at 75% (**Fig 4B**). The percentages of cells with off-center TCR clusters and asymmetrical pSMAC structures also stayed at 25-30% throughout the observation period (**Fig 4A, OKT3+ICAM-1:**

363 **asymmetrical and Fig 4B**).

364 In contrast, on the SLBs with HIV gp120, OKT3 and ICAM-1, only 17% of the
365 cells displayed mature synapses with central TCR clusters at 30 minutes, although at 10
366 minutes the proportion was comparable to that in the absence of gp120 (**Fig 4A,**
367 **gp120+OKT3+ICAM-1: symmetrical and Fig. 4B**). Hence, after 30 minutes, the
368 number of cells with mature synapses on the SLBs with gp120 declined. Most of the
369 cells became elongated with off-center TCR clusters and no longer had well-defined
370 ICAM-1 rings (**Fig 4A, gp120+OKT3+ICAM-1: asymmetrical**), indicative of cells that
371 had resumed migration. These data demonstrate that the presence of HIV gp120 not
372 only alters TCR accumulation but also affects the propensity of the cells to migrate after
373 forming the synapses.

374

375 **Sustained Lck phosphorylation in the synapse in the presence of HIV gp120**

376 Given the ability of HIV gp120 to enhance TCR accumulation in the synapse, we
377 next evaluated whether HIV gp120 affected the activation of TCR-proximal signaling.
378 Since Lck activation is the first signal triggered upon TCR engagement and by gp120-
379 CD4 binding (18, 29, 45, 46), we performed immunostaining of CD4 T cells interacting
380 with OKT3 and ICAM-1 plus or minus gp120 on the SLBs with anti-Lck antibodies. The
381 cells were added to the SLBs for 10 or 45 minutes, fixed, permeabilized, and stained
382 with antibodies specific for total Lck, pLck (Y505), and pLck (Y394) (**Fig 5**). TIRFM was
383 then used to detect Lck phosphorylation and its recruitment to the synapses. TIRFM
384 allows the detection of fluorescence within a 100-200 nm slice and thus provides high
385 lateral and axial resolution of Lck or pLck signals recruited specifically to the membrane-

386 proximal areas at the T cell-bilayer interface (<200 nm of the T cell plasma membranes
387 at the cell-bilayer contact sites). The fluorescence signals beyond this thin area are
388 excluded from the measurements. The data from individual cells from one of the donors
389 are shown in **Fig 5A**, while the cumulative data from three different donors tested in
390 separate experiments are presented in **Fig 5B**.

391 In the cells on the control OKT3+ICAM-1 SLBs with no gp120, total Lck levels at
392 the synapses were comparable at 10 minutes and 45 minutes (**Fig 5A-B**). In the
393 presence of HIV gp120 a slightly higher level of total Lck staining was observed at 10
394 minutes, but overall the total Lck staining remained relatively constant over time in the
395 presence or absence of HIV gp120. In contrast, phosphorylated Lck staining (both
396 pY505 and pY394) showed a declining trend from 10 minutes to 45 minutes in the cells
397 on the control SLBs. This is consistent with the fact that the physiologic Lck activation
398 triggered via TCR is transient (18, 19, 46). In the presence of HIV gp120, however,
399 pLck(Y505) staining showed an altered pattern: it increased from 10 minutes to 45
400 minutes such that the pLck(Y505) staining at 45 minutes was higher in the presence vs.
401 absence of HIV gp120. pLck (Y394) staining did not rise from 10 minutes to 45 minutes
402 but was sustained at higher levels at both time points in the presence of HIV gp120.
403 **Fig 5C (middle and right panels)** further shows that, in the presence of HIV gp120,
404 most pLck staining accumulated at the cSMAC after 45 minutes and localized near
405 gp120 and OKT3. This pattern was not seen with the total Lck, which remained
406 dispersed as small puncta throughout the cell-bilayer contact areas (**Fig 5C left panel**),
407 indicating the vast majority of Lck molecules were not phosphorylated and were not
408 recruited to the membrane-proximal area of the gp120-containing cSMAC. In the

absence of gp120, pLck and total Lck also did not converge to the cSMAC or co-localize with OKT3, consistent with past data (29).

These data indicate that, unlike the transient Lck activation induced by TCR in the peripheral areas of the immunological synapse, the presence of HIV Env gp120 in the synapse triggers a sustained level of phosphorylated Lck which accumulates in the synapse along with gp120 and OKT3 for up to 45 minutes. This pattern is reminiscent of the long-lasting Lck activation induced by HIV gp120 alone (29) and suggests the dominant effects of HIV gp120 over TCR on Lck activation in the CD4 T cell immunological synapse.

HIV gp120-mediated enhancement of CD4 T cell activation and virus replication

The ability of HIV gp120 to augment TCR-induced Lck activation led us to investigate the downstream events associated with T cell activation. By itself HIV gp120 only partially activates the early TCR signaling machinery on CD4 T cells, and the signals do not propagate to result in intracellular Ca^{2+} elevation or increased CD69 expression (29). However, the presence of HIV gp120 during TCR engagement may alter CD4 T cell activation. To test this idea, we compared the extent of CD69 upregulation, IL-2 secretion, and proliferation when CD4 T cells were triggered by OKT3 or by a combination of OKT3 and HIV gp120. To accommodate for the prolonged assay periods required to detect CD69 upregulation and IL-2 secretion beyond the one hour period for the TIRFM experiments above, SLBs were formed on the standard 5-μm sterile silica beads and functionalized with OKT3, ICAM-1, and gp120 or no gp120, which were then incubated with CD4 T cells for up to 24 hours. SLB-beads coated with

OKT3, ICAM-1, and CD80 (a co-stimulatory molecule binding to CD28) or with only ICAM-1 were also tested for comparison. The beads have been shown to provide equivalent stimulation to T cells as the planar surfaces (47). The cells were stained with anti-CD69 mAb at 6 hours and 24 hours and analyzed by flow cytometry. The supernatants were collected at 24 hours and tested for IL-2 in ELISA. Untreated cells served as background control. T cell proliferation was also assessed based on CFSE dilution 5 days after the cells were cultured on wells coated with OKT3 with or without gp120.

On the CD4 T cells treated with OKT3 + ICAM1 beads, CD69 expression increased but declined rapidly (**Fig 6A**). Stimulation with OKT3 + ICAM-1 beads also induced no IL-2 production (**Fig 6B**). With the addition of HIV gp120, CD69 upregulation was augmented and sustained over the 24-hour observation period (**Fig 6A**). These results were comparable to those achieved with an OKT3 + CD80 co-stimulation. HIV gp120 also significantly increased IL-2 production to the levels observed with an OKT3 + CD80 co-stimulation (**Fig 6B**). Cells treated with ICAM-1-beads showed a similar response to untreated cells and did not upregulate CD69 expression or secrete IL-2. For CD4 T cell proliferation assay (**Fig 6C**), CFSE-labeled CD4 T cells were cultured for 5 days in wells coated with OKT3 plus or minus HIV gp120 (strains SF162 or CH040). Enhanced proliferation was observed with CD4 T cells stimulated with OKT3 plus HIV gp120 as compared with OKT3 alone, and the enhanced response was inhibited by the Leu3A mAb that blocked HIV gp120-CD4 binding. These results indicate that HIV Env gp120 enhanced CD4 T cell activation to a similar extent as the bona fide co-stimulatory ligand.

To determine whether the CD4 T cells stimulated by OKT3 in the presence of HIV gp120 can support virus infection better than those activated by OKT3 alone, we treated the activated cells with HIV-1 SF162 and measured virus replication based on virus p24 in the culture supernatants. For comparison, p24 levels were also measured in the supernatants of unstimulated cells that supported minimal virus replication. These experiments were done without addition of exogenous cytokines. The data show that the amounts of p24 produced by the stimulated cells increased from day 3 to day 10 post-infection, indicative of active virus replication, although the concentrations varied among the different donors (**Fig 6D**). Notably, higher levels of p24 were produced by infected CD4 T cells that had been stimulated with OKT3 in the presence of HIV gp120 than in those activated only with OKT3. The greater p24 production induced by OKT3 + HIV gp120 was detected as early as day 3 and became more evident at day 10. About 2-5 fold enhancement was attained in the absence of any exogenous cytokines and consistently observed with cells from the different donors. Importantly, virus replication after stimulation with OKT3 + HIV gp120 was comparable to or even higher than that seen in CD4 T cells stimulated with OKT3 and anti-CD28 mAb, indicating the HIV gp120's potent co-stimulatory activity. All together these results show that in the CD4 T cell immunological synapse HIV Env may act as a co-stimulator that heightens TCR activation of the CD4 T cells and imparts the cells with the capacity to support higher levels of virus replication.

476 **Discussion**

477 This study demonstrated the ability of HIV Env gp120 to alter the kinetics of TCR
478 recruitment and the activation of TCR-proximal signaling at the CD4 T cell
479 immunological synapse. While most earlier studies examine the changes in the
480 immunological synapse formed by the CD4 T cells already infected with the virus (48-
481 50), this study evaluated the HIV Env interaction with target CD4 T cells in the
482 immunological synapse prior to infection. Notably, the presence of the HIV Env did not
483 interfere with the immunological synapse assembly. TCR accumulation at the cSMAC
484 of the synapse and its segregation from the adhesive pSMAC ring of ICAM-1/LFA-1
485 interactions proceeded similarly in the presence or absence of the HIV Env. The
486 proportion of cells forming the synapse was also comparable. However, the binding of
487 HIV Env to CD4 T cells resulted in the accumulation of HIV Env and phosphorylated Lck
488 at the cSMAC, although the cSMAC is normally devoid of Lck in the absence of the HIV
489 Env (18, 19, 31). Importantly, the HIV Env accumulation at the synapse enhanced
490 TCR-induced activation that predisposed the target CD4 T cells to become more
491 receptive to HIV infection and productive replication. It should be noted that this activity
492 was observed with the HIV Env gp120 monomers that cannot mediate virus infection.
493 However, these monomeric gp120 proteins have receptor-binding activities. Moreover,
494 when bound on membranes like the SLBs, the HIV Env gp120 monomers were able to
495 cross-link and cluster the HIV Env-receptor interactions to the cSMAC to result in Lck
496 activation at the cSMAC. Past studies also have reported the activation of Lck and the
497 downstream signals upon CD4 engagement by the HIV virions or the HIV Env
498 expressed on cells (51-53). On the surfaces of virions and infected cells,

heterogeneous species of the HIV Env glycoproteins are expressed (54-56), including non-functional Env proteins that cannot partake in the virus entry process but may have immunomodulatory activities demonstrated in this study.

The exact mechanism by which the HIV Env at the immunological synapse augments TCR-induced activation of CD4 T cells is yet to be delineated. However, the temporal pattern of TCR recruitment was significantly different in the presence of the HIV Env. Thereby, in the presence of the HIV Env the TCR density in the synapse reached a higher peak (~3 fold higher than control) and declined over time. In contrast, in the absence of the HIV Env, the TCR level increased to a plateau that was maintained throughout the one hour observation time. The alteration of TCR mobilization was induced by the HIV Env binding to CD4 T cells. However, treatment with the anti-Env mAbs directed to the CD4-binding site, the V1V2 domain, or the V3 loop reduced the HIV Env accumulation in the CD4 T cell synapses, without blocking the enhanced TCR recruitment to the synapses. These data suggest the potential involvement of multiple receptors in affecting the TCR recruitment and that a single anti-Env mAb is not sufficient to block this activity. We also observed that none of the individual anti-Env mAbs, including the 654 mAb efficiently blocking CD4-gp120 interaction, was able to totally prevent the HIV Env recruitment to the CD4 T cell synapses. Moreover, low levels of HIV Env were found to interact with the CD8 T cells on the SLBs, albeit without affecting the TCR recruitment. Hence, in addition to CD4, the other HIV Env receptors such as the integrin α4β7 and the mannose receptors are likely to be engaged at these synapses. Further, given that a partial inhibition of the Env recruitment was also seen with a mAb against the V3 loop known to be important

for the chemokine receptor binding (57), these co-receptors may also play a role in the synapses. Nonetheless, the relative contributions of the different non-CD4 receptors remain to be determined.

The activity of the HIV Env to enhance TCR-induced T cell activation is rather unique and is in contrast to the inhibitory effects seen more commonly with other virus proteins. For example, the presence of HERV Env on dendritic cells reduces the ability of the dendritic cells to form immunological synapses with T cells resulting in blockage of T cell activation (58). Similarly, the Nef proteins of most SIV and HIV-2 have been shown to downregulate TCR and CD3 expression in virus-infected T cells resulting in the suppression of immunological synapse formation with antigen presenting cells (48). In contrast, the HIV-1 Nef expression in infected CD4 T cells does not disrupt the formation of immunological synapses between the infected CD4 T cells and APCs and instead affects the synapse functions by inhibiting TCR-induced actin polymerization and TCR-proximal signaling (48, 59). The HCMV pUL125 protein also reduces the efficiency of the immunological synapse formation by modifying the actin cytoskeleton required for the formation of immunological synapses with NK cells (60). Alternatively, the hRSV nucleoprotein interferes with the assembly of the dendritic cell-CD4 T cell immunological synapses by decreasing TCR-pMHC binding and TCR-proximal signaling (61). The ability of these viruses to directly tamper with the immunological synapse and suppress immune cell activation serves as an escape mechanism from immune surveillance. By contrast, HIV via its Env manipulates the immunological synapse to optimize the activation state of the uninfected CD4 T cells to increase the capacity of these cells to support virus replication.

545 Although the significance of the HIV Env-induced alterations affecting the kinetics
546 of TCR recruitment and retention in the immunological synapse is not fully understood,
547 the data from this study show that the TCR accumulation at the cSMAC was
548 accompanied by HIV Env recruitment to the same central area of the synapse. In our
549 earlier studies, HIV Env-CD4 interactions were also found to be mobilized to the
550 synapse center to form a cSMAC-like structure independent of TCR engagement (28,
551 29). Importantly, the central Env-CD4 clusters were associated with long-lasting but
552 partial activation of membrane-proximal signals that began with Lck phosphorylation
553 (29). The present study also showed a similar pattern of durable Lck activation in the
554 Env-containing TCR-induced immunological synapse. These observations indicate the
555 dominant effect of the Env over the transient TCR-induced signaling.
556 The presence of HIV Env also enhanced TCR-induced CD4 T cell activation, as
557 measured by CD69 upregulation and IL-2 secretion, and induced a greater level of CD4
558 T cell proliferation. These results are in concordance with a previous report by
559 Zimmermann et al. (62) showing that a simultaneous engagement of TCR by anti-CD3
560 antibody and CD4 by the HIV Env boosted CD4 T cell activation. In contrast, the
561 interaction of CD4 T cells with soluble HIV gp120 retarded TCR-induced proliferation.
562 HIV Env-CD4 interactions that occurred separately prior to TCR engagement were also
563 found to undermine TCR-proximal signaling and downstream activation events (62).
564 Similarly, the pre-engagement of CD4 by HIV followed by treatment with anti-
565 CD3/CD28-coated beads resulted in the inhibition of Lck and F-actin recruitment to the
566 T cell immunological synapses (49). Taken together, these studies present evidence for
567 the multifaceted role of the HIV Env in shaping the activation state and functionality of

568 the host CD4 T cells. It is also important to note that such HIV Env-mediated immune-
569 modulation may play a part not only in the immune dysregulation seen during HIV
570 infection, but also in the inadequate elicitation and maturation of effector and memory
571 immune responses to many HIV Env-based vaccine candidates evaluated thus far (63-
572 65).

573 This study demonstrated the contribution of the HIV Env as would be expressed
574 on virus-bearing APCs in augmenting the TCR-induced activation of cognate CD4 T
575 cells that are targeted by the virus. We also observed that the HIV Env reduced the
576 duration of the otherwise long-lasting immunological synapse, consistent with the
577 transient nature of T cell migration arrest induced by the HIV Env reported previously
578 (28). A transient synapse may offer advantages for the virus. After a brief migration
579 arrest to allow cell-cell contact and virus transfer, a subsequent rapid detachment would
580 prevent cell-cell fusion that terminates the virus life cycle while promoting the spread of
581 the newly infected cells to other sites in the lymphoid tissues. Overall, the data
582 presented herein offers a model in which HIV, via its Env glycoproteins, alters the
583 immunologic synapse and the activation state of CD4 T cells undergoing TCR activation
584 in a way that is likely to facilitate viral replication and spread.
585

Acknowledgements

We thank Michael Cammer for assistance with data analysis, Jianping Liu and Kathleen C. Prins for conducting pilot experiments, Radhika Wikramanayake for editing the manuscript, Susan Zolla-Pazner, Constance Williams and Vincenza Itri for providing the monoclonal antibodies used in the study and Michael Tuen for general lab support.

This study was supported with funds from the Research Career Scientist Award (CEH) and Merit Review Award (CEH) from the Department of Veterans Affairs (VA), Veterans Health Administration, Office of Research and Development and by NIH grants AI093210, AI100151 and AI102740 (CEH). The funders had no role in study design, data collection and interpretation, or the decision to submit the work for publication.

References

1. **Clerici M, Stocks NI, Zajac RA, Boswell RN, Lucey DR, Via CS, Shearer GM.** 1989. Detection of three distinct patterns of T helper cell dysfunction in asymptomatic, human immunodeficiency virus-seropositive patients. Independence of CD4+ cell numbers and clinical staging. J Clin Invest **84:**1892-1899.
2. **McCune JM.** 2001. The dynamics of CD4+ T-cell depletion in HIV disease. Nature **410:**974-979.
3. **Bleul CC, Wu L, Hoxie JA, Springer TA, Mackay CR.** 1997. The HIV coreceptors CXCR4 and CCR5 are differentially expressed and regulated on human T lymphocytes. Proc Natl Acad Sci U S A **94:**1925-1930.
4. **Lee B, Sharron M, Montaner LJ, Weissman D, Doms RW.** 1999. Quantification of CD4, CCR5, and CXCR4 levels on lymphocyte subsets, dendritic cells, and differentially conditioned monocyte-derived macrophages. Proc Natl Acad Sci U S A **96:**5215-5220.
5. **Korin YD, Zack JA.** 1998. Progression to the G1b phase of the cell cycle is required for completion of human immunodeficiency virus type 1 reverse transcription in T cells. J Virol **72:**3161-3168.
6. **Zack JA, Haislip AM, Krogstad P, Chen IS.** 1992. Incompletely reverse-transcribed human immunodeficiency virus type 1 genomes in quiescent cells can function as intermediates in the retroviral life cycle. J Virol **66:**1717-1725.
7. **Sun Y, Pinchuk LM, Agy MB, Clark EA.** 1997. Nuclear import of HIV-1 DNA in resting CD4+ T cells requires a cyclosporin A-sensitive pathway. J Immunol **158:**512-517.
8. **Stevenson M, Stanwick TL, Dempsey MP, Lamonica CA.** 1990. HIV-1 replication is controlled at the level of T cell activation and proviral integration. EMBO J **9:**1551-1560.
9. **Hiscott J, Kwon H, Genin P.** 2001. Hostile takeovers: viral appropriation of the NF-kappaB pathway. J Clin Invest **107:**143-151.
10. **Shannon B, Yi TJ, Thomas-Pavanel J, Chieza L, Janakiram P, Saunders M, Tharao W, Huibner S, Remis R, Rebbapragada A, Kaul R.** 2014. Impact of asymptomatic herpes simplex virus type 2 infection on mucosal homing and immune cell subsets in the blood and female genital tract. J Immunol **192:**5074-5082.
11. **McKinnon LR, Izulla P, Nagelkerke N, Munyao J, Wanjiru T, Shaw SY, Gichuki R, Kariuki C, Muriuki F, Musyoki H, Gakii G, Gelmon L, Kaul R, Kimani J.** 2015. Risk Factors for HIV Acquisition in a Prospective Nairobi-Based Female Sex Worker Cohort. AIDS Behav **19:**2204-2213.
12. **Wasserheit JN.** 1992. Epidemiological synergy. Interrelationships between human immunodeficiency virus infection and other sexually transmitted diseases. Sex Transm Dis **19:**61-77.
13. **Carnathan DG, Wetzel KS, Yu J, Lee ST, Johnson BA, Paiardini M, Yan J, Morrow MP, Sardesai NY, Weiner DB, Ertl HC, Silvestri G.** 2015. Activated CD4+CCR5+ T cells in the rectum predict increased SIV acquisition in SIVGag/Tat-vaccinated rhesus macaques. Proc Natl Acad Sci U S A **112:**518-523.
14. **Goode D, Truong R, Villegas G, Calenda G, Guerra-Perez N, Piatak M, Lifson JD, Blanchard J, Gettie A, Robbiani M, Martinelli E.** 2014. HSV-2-driven increase in the expression of alpha4beta7 correlates with increased susceptibility to vaginal SHIV(SF162P3) infection. PLoS Pathog **10:**e1004567.
15. **Fooksman DR, Vardhana S, Vasiliver-Shamis G, Liese J, Blair DA, Waite J, Sacristan C, Victora GD, Zanin-Zhorov A, Dustin ML.** 2010. Functional anatomy of T cell activation and synapse formation. Annu Rev Immunol **28:**79-105.
16. **Huppa JB, Davis MM.** 2003. T-cell-antigen recognition and the immunological synapse. Nat Rev Immunol **3:**973-983.

17. **Dustin ML, Bromley SK, Kan Z, Peterson DA, Unanue ER.** 1997. Antigen receptor engagement delivers a stop signal to migrating T lymphocytes. Proc Natl Acad Sci U S A **94:**3909-3913.
18. **Campi G, Varma R, Dustin ML.** 2005. Actin and agonist MHC-peptide complex-dependent T cell receptor microclusters as scaffolds for signaling. J Exp Med **202:**1031-1036.
19. **Varma R, Campi G, Yokosuka T, Saito T, Dustin ML.** 2006. T cell receptor-proximal signals are sustained in peripheral microclusters and terminated in the central supramolecular activation cluster. Immunity **25:**117-127.
20. **Choudhuri K, Llodra J, Roth EW, Tsai J, Gordo S, Wucherpfennig KW, Kam LC, Stokes DL, Dustin ML.** 2014. Polarized release of T-cell-receptor-enriched microvesicles at the immunological synapse. Nature **507:**118-123.
21. **Martin N, Welsch S, Jolly C, Briggs JA, Vaux D, Sattentau QJ.** 2010. Virological synapse-mediated spread of human immunodeficiency virus type 1 between T cells is sensitive to entry inhibition. J Virol **84:**3516-3527.
22. **Do T, Murphy G, Earl LA, Del Prete GQ, Grandinetti G, Li GH, Estes JD, Rao P, Trubey CM, Thomas J, Spector J, Bliss D, Nath A, Lifson JD, Subramaniam S.** 2014. Three-dimensional imaging of HIV-1 virological synapses reveals membrane architectures involved in virus transmission. J Virol **88:**10327-10339.
23. **Hubner W, McNerney GP, Chen P, Dale BM, Gordon RE, Chuang FY, Li XD, Asmuth DM, Huser T, Chen BK.** 2009. Quantitative 3D video microscopy of HIV transfer across T cell virological synapses. Science **323:**1743-1747.
24. **Jolly C, Kashefi K, Hollinshead M, Sattentau QJ.** 2004. HIV-1 cell to cell transfer across an Env-induced, actin-dependent synapse. J Exp Med **199:**283-293.
25. **Rudnicka D, Feldmann J, Porrot F, Wietgrefe S, Guadagnini S, Prevost MC, Estaquier J, Haase AT, Sol-Foulon N, Schwartz O.** 2009. Simultaneous cell-to-cell transmission of human immunodeficiency virus to multiple targets through polysynapses. J Virol **83:**6234-6246.
26. **Chen P, Hubner W, Spinelli MA, Chen BK.** 2007. Predominant mode of human immunodeficiency virus transfer between T cells is mediated by sustained Env-dependent neutralization-resistant virological synapses. J Virol **81:**12582-12595.
27. **Vasiliver-Shamis G, Dustin ML, Hioe CE.** 2010. HIV-1 Virological Synapse is not Simply a Copycat of the Immunological Synapse. Viruses **2:**1239-1260.
28. **Vasiliver-Shamis G, Tuen M, Wu TW, Starr T, Cameron TO, Thomson R, Kaur G, Liu J, Visciano ML, Li H, Kumar R, Ansari R, Han DP, Cho MW, Dustin ML, Hioe CE.** 2008. Human immunodeficiency virus type 1 envelope gp120 induces a stop signal and virological synapse formation in noninfected CD4+ T cells. J Virol **82:**9445-9457.
29. **Vasiliver-Shamis G, Cho MW, Hioe CE, Dustin ML.** 2009. Human immunodeficiency virus type 1 envelope gp120-induced partial T-cell receptor signaling creates an F-actin-depleted zone in the virological synapse. J Virol **83:**11341-11355.
30. **Yokosuka T, Kobayashi W, Sakata-Sogawa K, Takamatsu M, Hashimoto-Tane A, Dustin ML, Tokunaga M, Saito T.** 2008. Spatiotemporal regulation of T cell costimulation by TCR-CD28 microclusters and protein kinase C theta translocation. Immunity **29:**589-601.
31. **Kao H, Lin J, Littman DR, Shaw AS, Allen PM.** 2008. Regulated movement of CD4 in and out of the immunological synapse. J Immunol **181:**8248-8257.
32. **Hioe CE, Tuen M, Vasiliver-Shamis G, Alvarez Y, Prins KC, Banerjee S, Nadas A, Cho MW, Dustin ML, Kachlany SC.** 2011. HIV envelope gp120 activates LFA-1 on CD4 T-lymphocytes and increases cell susceptibility to LFA-1-targeting leukotoxin (LtxA). PLoS One **6:**e23202.
33. **Beal AM, Anikeeva N, Varma R, Cameron TO, Norris PJ, Dustin ML, Sykulev Y.** 2008. Protein kinase C theta regulates stability of the peripheral adhesion ring junction and contributes to the sensitivity of target cell lysis by CTL. J Immunol **181:**4815-4824.

34. **Gross CC, Brzostowski JA, Liu D, Long EO.** 2010. Tethering of intercellular adhesion molecule on target cells is required for LFA-1-dependent NK cell adhesion and granule polarization. J Immunol **185:**2918-2926.
35. **Prins KC, Vasiliver-Shamis G, Cammer M, Depoil D, Dustin ML, Hioe CE.** 2012. Imaging of HIV-1 envelope-induced virological synapse and signaling on synthetic lipid bilayers. J Vis Exp.
36. **DeSantis MC, Kim JH, Song H, Klasse PJ, Cheng W.** 2016. Quantitative Correlation between Infectivity and Gp120 Density on HIV-1 Virions Revealed by Optical Trapping Virometry. The Journal of biological chemistry **291:**13088-13097.
37. **Zhu P, Liu J, Bess J, Jr., Chertova E, Lifson JD, Grise H, Ofek GA, Taylor KA, Roux KH.** 2006. Distribution and three-dimensional structure of AIDS virus envelope spikes. Nature **441:**847-852.
38. **Hermida-Matsumoto L, Resh MD.** 2000. Localization of human immunodeficiency virus type 1 Gag and Env at the plasma membrane by confocal imaging. J Virol **74:**8670-8679.
39. **Nydegger S, Khurana S, Krementsov DN, Foti M, Thali M.** 2006. Mapping of tetraspanin-enriched microdomains that can function as gateways for HIV-1. The Journal of cell biology **173:**795-807.
40. **Hioe CE, Hildreth JE, Zolla-Pazner S.** 1999. Enhanced HIV type 1 neutralization by human anti-glycoprotein 120 monoclonal antibodies in the presence of monoclonal antibodies to lymphocyte function-associated molecule 1. AIDS Res Hum Retroviruses **15:**523-531.
41. **Hioe CE, Wrin T, Seaman MS, Yu X, Wood B, Self S, Williams C, Gorny MK, Zolla-Pazner S.** 2010. Anti-V3 monoclonal antibodies display broad neutralizing activities against multiple HIV-1 subtypes. PLoS One **5:**e10254.
42. **Upadhyay C, Mayr LM, Zhang J, Kumar R, Gorny MK, Nadas A, Zolla-Pazner S, Hioe CE.** 2014. Distinct mechanisms regulate exposure of neutralizing epitopes in the V2 and V3 loops of HIV-1 envelope. J Virol **88:**12853-12865.
43. **Li L, Wang XH, Williams C, Volsky B, Steczko O, Seaman MS, Luthra K, Nyambi P, Nadas A, Giudicelli V, Lefranc MP, Zolla-Pazner S, Gorny MK.** 2015. A broad range of mutations in HIV-1 neutralizing human monoclonal antibodies specific for V2, V3, and the CD4 binding site. Molecular immunology **66:**364-374.
44. **Levine BL, Bernstein WB, Connors M, Craighead N, Lindsten T, Thompson CB, June CH.** 1997. Effects of CD28 costimulation on long-term proliferation of CD4+ T cells in the absence of exogenous feeder cells. J Immunol **159:**5921-5930.
45. **Briant L, Robert-Hebmann V, Acquaviva C, Pelchen-Matthews A, Marsh M, Devaux C.** 1998. The protein tyrosine kinase p56lck is required for triggering NF-kappaB activation upon interaction of human immunodeficiency virus type 1 envelope glycoprotein gp120 with cell surface CD4. J Virol **72:**6207-6214.
46. **Ziemba SE, Menard SL, McCabe MJ, Jr., Rosenspire AJ.** 2009. T-cell receptor signaling is mediated by transient Lck activity, which is inhibited by inorganic mercury. FASEB J **23:**1663-1671.
47. **Crites TJ, Padhan K, Muller J, Krogsgaard M, Gudla PR, Lockett SJ, Varma R.** 2014. TCR Microclusters pre-exist and contain molecules necessary for TCR signal transduction. J Immunol **193:**56-67.
48. **Arhel N, Lehmann M, Clauss K, Nienhaus GU, Piguet V, Kirchhoff F.** 2009. The inability to disrupt the immunological synapse between infected human T cells and APCs distinguishes HIV-1 from most other primate lentiviruses. J Clin Invest **119:**2965-2975.
49. **Nyakeriga AM, Fichtenbaum CJ, Goebel J, Nicolaou SA, Conforti L, Chougnet CA.** 2009. Engagement of the CD4 receptor affects the redistribution of Lck to the immunological synapse in primary T cells: implications for T-cell activation during human immunodeficiency virus type 1 infection. J Virol **83:**1193-1200.

50. **Thoulouze MI, Sol-Foulon N, Blanchet F, Dautry-Varsat A, Schwartz O, Alcover A.** 2006. Human immunodeficiency virus type-1 infection impairs the formation of the immunological synapse. Immunity **24:**547-561.
51. **Tian H, Lempicki R, King L, Donoghue E, Samelson LE, Cohen DI.** 1996. HIV envelope-directed signaling aberrancies and cell death of CD4+ T cells in the absence of TCR co-stimulation. International immunology **8:**65-74.
52. **Popik W, Pitha PM.** 1996. Binding of human immunodeficiency virus type 1 to CD4 induces association of Lck and Raf-1 and activates Raf-1 by a Ras-independent pathway. Molecular and cellular biology **16:**6532-6541.
53. **Briand G, Barbeau B, Tremblay M.** 1997. Binding of HIV-1 to its receptor induces tyrosine phosphorylation of several CD4-associated proteins, including the phosphatidylinositol 3-kinase. Virology **228:**171-179.
54. **Tong T, Osawa K, Robinson JE, Crooks ET, Binley JM.** 2013. Topological analysis of HIV-1 glycoproteins expressed in situ on virus surfaces reveals tighter packing but greater conformational flexibility than for soluble gp120. J Virol **87:**9233-9249.
55. **Crooks ET, Tong T, Osawa K, Binley JM.** 2011. Enzyme digests eliminate nonfunctional Env from HIV-1 particle surfaces, leaving native Env trimers intact and viral infectivity unaffected. J Virol **85:**5825-5839.
56. **Leaman DP, Zwick MB.** 2013. Increased functional stability and homogeneity of viral envelope spikes through directed evolution. PLoS Pathog **9:**e1003184.
57. **Cashin K, Paukovics G, Jakobsen MR, Ostergaard L, Churchill MJ, Gorry PR, Flynn JK.** 2014. Differences in coreceptor specificity contribute to alternative tropism of HIV-1 subtype C for CD4(+) T-cell subsets, including stem cell memory T-cells. Retrovirology **11:**97.
58. **Hummel J, Kammerer U, Muller N, Avota E, Schneider-Schaulies S.** 2015. Human endogenous retrovirus envelope proteins target dendritic cells to suppress T-cell activation. Eur J Immunol **45:**1748-1759.
59. **Abraham L, Bankhead P, Pan X, Engel U, Fackler OT.** 2012. HIV-1 Nef limits communication between linker of activated T cells and SLP-76 to reduce formation of SLP-76-signaling microclusters following TCR stimulation. J Immunol **189:**1898-1910.
60. **Stanton RJ, Prod'homme V, Purbhoo MA, Moore M, Aicheler RJ, Heinzmann M, Bailer SM, Haas J, Antrobus R, Weekes MP, Lehner PJ, Vojtesek B, Miners KL, Man S, Wilkie GS, Davison AJ, Wang EC, Tomasec P, Wilkinson GW.** 2014. HCMV pUL135 remodels the actin cytoskeleton to impair immune recognition of infected cells. Cell Host Microbe **16:**201-214.
61. **Cespedes PF, Bueno SM, Ramirez BA, Gomez RS, Riquelme SA, Palavecino CE, Mackern-Oberti JP, Mora JE, Depoil D, Sacristan C, Cammer M, Creneguy A, Nguyen TH, Riedel CA, Dustin ML, Kalergis AM.** 2014. Surface expression of the hRSV nucleoprotein impairs immunological synapse formation with T cells. Proc Natl Acad Sci U S A **111:**E3214-3223.
62. **Zimmermann K, Liechti T, Haas A, Rehr M, Trkola A, Gunthard HF, Oxenius A.** 2015. The orientation of HIV-1 gp120 binding to the CD4 receptor differentially modulates CD4+ T cell activation. J Immunol **194:**637-649.
63. **Fouda GG, Cunningham CK, McFarland EJ, Borkowsky W, Muresan P, Pollara J, Song LY, Liebl BE, Whitaker K, Shen X, Vandergrift NA, Overman RG, Yates NL, Moody MA, Fry C, Kim JH, Michael NL, Robb M, Pitisuttithum P, Kaewkungwal J, Nitayaphan S, Rerks-Ngarm S, Liao HX, Haynes BF, Montefiori DC, Ferrari G, Tomaras GD, Permar SR.** 2015. Infant HIV type 1 gp120 vaccination elicits robust and durable anti-V1V2 immunoglobulin G responses and only rare envelope-specific immunoglobulin A responses. J Infect Dis **211:**508-517.
64. **Haynes BF, Gilbert PB, McElrath MJ, Zolla-Pazner S, Tomaras GD, Alam SM, Evans DT, Montefiori DC, Karnasuta C, Sutthent R, Liao HX, DeVico AL, Lewis GK, Williams C, Pinter A,**

Fong Y, Janes H, DeCamp A, Huang Y, Rao M, Billings E, Karasavvas N, Robb ML, Ngauy V, de Souza MS, Paris R, Ferrari G, Bailer RT, Soderberg KA, Andrews C, Berman PW, Frahm N, De Rosa SC, Alpert MD, Yates NL, Shen X, Koup RA, Pitisuttithum P, Kaewkungwal J, Nitayaphan S, Rerks-Ngarm S, Michael NL, Kim JH. 2012. Immune-correlates analysis of an HIV-1 vaccine efficacy trial. N Engl J Med **366:**1275-1286.

65. **Yates NL, Liao HX, Fong Y, deCamp A, Vandergrift NA, Williams WT, Alam SM, Ferrari G, Yang ZY, Seaton KE, Berman PW, Alpert MD, Evans DT, O'Connell RJ, Francis D, Sinangil F, Lee C, Nitayaphan S, Rerks-Ngarm S, Kaewkungwal J, Pitisuttithum P, Tartaglia J, Pinter A, Zolla-Pazner S, Gilbert PB, Nabel GJ, Michael NL, Kim JH, Montefiori DC, Haynes BF, Tomaras GD.** 2014. Vaccine-induced Env V1-V2 IgG3 correlates with lower HIV-1 infection risk and declines soon after vaccination. Sci Transl Med **6:**228ra239.

Figure legends

Fig 1: Recruitment of HIV Env gp120 and TCR to the CD4 and CD8 T cell immunological synapses. (**A-B**) Activated CD4 T cells were introduced to SLBs containing fluorescence-tagged anti-CD3 antibody OKT3, ICAM-1, and gp120 or no gp120. Images of the cell contact area (as measured by interference reflection microscopy or IRM) and fluorescence signals were collected for one hour. (**A**) Representative images from the 10-minute time point are shown. Merge: combined fluorescence signals from OKT3 and gp120. White bar: 5 μm. **(B)** The distribution of gp120 (left) and TCR (right) in the CD4 T cell synapse at the 10-minute time point. The densities of gp120 and OKT3 were measured radially from the center of each of 30 cells per experiment (white circle in panel A merge, top). Data from representative cells are shown in the top right and left panels. The averages and standard errors from experiments performed independently with cells from three different donors (>30 cells per experiment) are shown in the bottom right and left panels. p values by the Mann Whitney test. (**C-D**) Activated CD8 T cells were added onto SLBs presenting anti-CD3 mAb OKT3, ICAM-1, and gp120 or no gp120. Live images were acquired for one hour. Data from the 10-minute time point were analyzed. (**C**) Images from representative CD8 T cells on SLBs with or without gp120. IRM: interference reflection microscopy. Merge: combined fluorescence signals from gp120 and OKT3. (**D**) The densities of gp120 (left) and OKT3 (right) were measured along the cell radius as above. Data from representative cells are shown in the top right and left panels. The averages and standard errors from three different donors were similarly calculated and shown in the bottom right and left panels. ns: not significant by the Mann Whitney test.

824

825 **Fig 2: Kinetics of TCR accumulation in the CD4 T cell immunological synapse in**
826 **the presence or absence of HIV Env gp120.** Activated CD4 T cells were introduced
827 to SLBs containing OKT3, ICAM-1, and plus or minus gp120. Live images were
828 collected for one hour. (**A**) Representative images from different time points during the
829 one-hour observation. Time points (green numbers) are in minutes. IRM: interference
830 reflection microscopy (contact area). Merge: combined fluorescence signals from
831 gp120 and OKT3. White bar: 5 μm. (**B**) The kinetics of OKT3 recruitment into the
832 synapse in the cells interacting with gp120 or no gp120 on the SLBs. The OKT3
833 densities were analyzed for ~30 individual cells per condition for up to 50 minutes. The
834 averages and standard deviations from all cells analyzed are shown in the left panel,
835 while data from randomly selected individual cells are shown in the right panel. The
836 data from two donors are presented. Statistical analysis was done with two-tailed non-
837 parametric Wilcoxon test comparing OKT3 recruitment in the presence versus absence
838 of HIV gp120. (**C**) The recruitment of gp120 to the synapse over time in cells interacting
839 with gp120, OKT3, and ICAM-1 on the SLBs. The gp120 densities were analyzed as
840 performed for OKT3. The left panel shows the averages and standard deviations from
841 ~30 cells and the right panel shows the patterns displayed by representative individual
842 cells. The data from two donors tested in independent experiments are shown.

843

844 **Fig 3: Reduction of HIV Env gp120 versus TCR accumulation by human anti-**
845 **gp120 mAbs.** Activated human CD4 T cells were introduced into SLBs with gp120, anti-
846 CD3 mAb OKT3 and ICAM-1 pre-treated with anti-gp120 mAbs that target the CD4-

847 binding site (654), V2 (2158), and V3 (2558), or an irrelevant mAb (1418). The mAbs
848 were used at 10 μg/ml, a saturating concentration for binding gp120 on the SLBs (28).
849 Cells were fixed at 20 minutes and images were collected. At least 30 cells were
850 analyzed for each condition. Statistical analysis was performed with one-way ANOVA.
851 Data from one of three independent experiments are shown. (**A**) The densities of
852 gp120 in the cell contact areas. ****, $p < 0.0001$; ***, $p < 0.001$; ns: not significant. Red
853 bars: mean values. (**B**) The densities of OKT3 in the cell contact areas. ***, $p < 0.001$
854 as compared to gp120 + OKT3 + ICAM plus or minus mAb; ns: not significant. Red
855 bars: mean values. (**C**) Representative images to show the distribution of gp120 and
856 OKT3 with or without anti-gp120 mAb. IRM: interference reflection microscopy to
857 determine the cell contact area. Merge: combined fluorescence signals from gp120 and
858 OKT3.
859
860 **Fig 4: Alteration of CD4 T cell synapse morphology over time in the presence of**
861 **HIV Env gp120.** Activated CD4 T cells were introduced to SLBs containing OKT3,
862 ICAM-1, and gp120 or no gp120 and monitored over time for changes in the synapse
863 morphology. (**A**). Representative images showing cells forming symmetrical versus
864 asymmetrical synapses as determined by the OKT3 cluster position relative to the
865 center of the cell. IRM: interference reflection microscopy. BF: bright field. Merge:
866 merged images from gp120, OKT3 and BF. White bar: 5 μm. (**B**) The percentages of
867 cells forming symmetrical or asymmetrical synapses at 10-minute and 30-minute time
868 points on SLBs with or without gp120. The averages (shown by bar graphs) from
869 independent experiments performed with cells from five different donors (depicted by

the scatter plots) are shown. *, p < 0.05 by one-way ANOVA with Dunn's multiple comparison.

Fig 5: Altered Lck activation in CD4 T cell immunological synapse in the presence of HIV Env gp120. CD4 T cells were introduced onto SLBs containing anti-CD3 mAb OKT3, ICAM-1, and gp120 or no gp120. After 10 minutes or 45 minutes, the cells were fixed and stained for total Lck, pLck (Y505), and pLck (Y394). The integrated fluorescence intensities detected by TIRFM was measured. (**A**) A total of 30 to 50 cells were analyzed for each condition and the data from one representative donor are shown. (**B**) The average integrated intensities from independent experiments performed with cells from three different donors are shown. ****, p <0.0001, ***, p <0.001, **, p <0.01, * <0.05, ns: not significant. Red bars: mean values. Iso Ctrl: staining with isotype control. Total and phosphorylated Lck staining at 10 minutes and 45 minutes in the presence or absence of gp120 was significantly higher than isotype control (p >0.05). Statistical analysis was performed with two-tailed *t*-tests. (**C**) Images of representative cells on SLBs with gp120 or without gp120 to show the distribution of total Lck and phosphorylated Lck at the two time points. IRM: interference reflection microscopy. Merge: merged gp120, OKT3, and Lck signals.

Fig. 6: Enhanced TCR-induced activation in the presence of HIV Env gp120. CD4 T cells were incubated with silica beads coated with the SLBs containing OKT3, ICAM-1, and gp120 or no gp120. Cells were also treated with beads coated with SLBs containing OKT3, ICAM-1 and CD80 or ICAM-1 alone for comparison. Untreated cells

were used to establish the background levels. CD4 T cells were initially activated on plates coated with anti-CD3 and anti-28 antibodies, and tested >7 days after activation. (**A**) After 6 and 24 hours of incubation with the SLB-coated beads, the cells were fixed, stained with anti-CD69 mAb, and analyzed by flow cytometry. (**B**) The culture supernatants were also collected after 24 hours of incubation and tested in ELISA for IL-2 secretion. The averages and standard errors shown in the graphs are from three experiments performed independently with cells from different donors. (**C**) CFSE dilution assay on CD4 T cells cultured for 5 days in wells coated with OKT3 plus or minus HIV gp120 (strains SF162 or CH040). CD4 T cells freshly isolated from PBMCs were used in the experiments. Anti-CD4 mAb Leu3a blocking CD4-gp120 binding was used to affirm the gp120-mediated enhancement. Histograms from one representative experiment are shown. Division indexes were calculated from the histograms with FlowJo; the means and standard errors from 2-5 independent experiments with cells from different donors are shown. Statistical analysis was done with the Mann Whitney test. (**D**) Virus production in cultures of CD4 T cells grown in wells coated with OKT3, OKT3+HIV gp120, or OKT3+anti-CD28 mAb for 5 days and infected with HIV-1 SF162. CD4 T cells freshly isolated from PBMCs were used in the experiments. Virus p24 concentrations in the supernatants were measured by ELISA on day 3 and day 10 post-infection. Data from the different donors are shown. Bkgrd: p24 concentrations in the supernatants of unstimulated cells. ****, $p < 0.0001$, **, $p < 0.01$, * < 0.05, ns: not significant.

Journal of Virology

Fig. 1

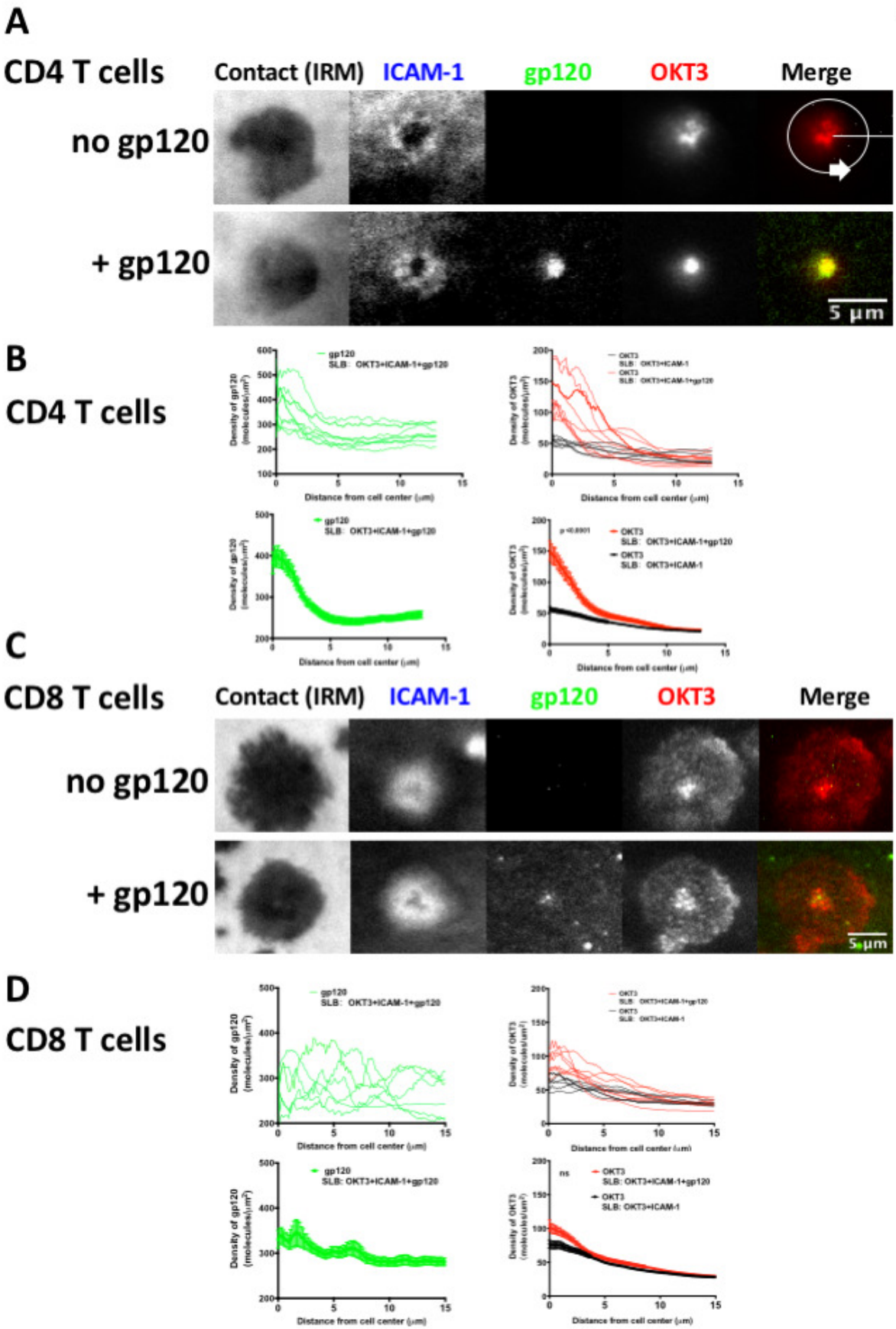

Fig. 2

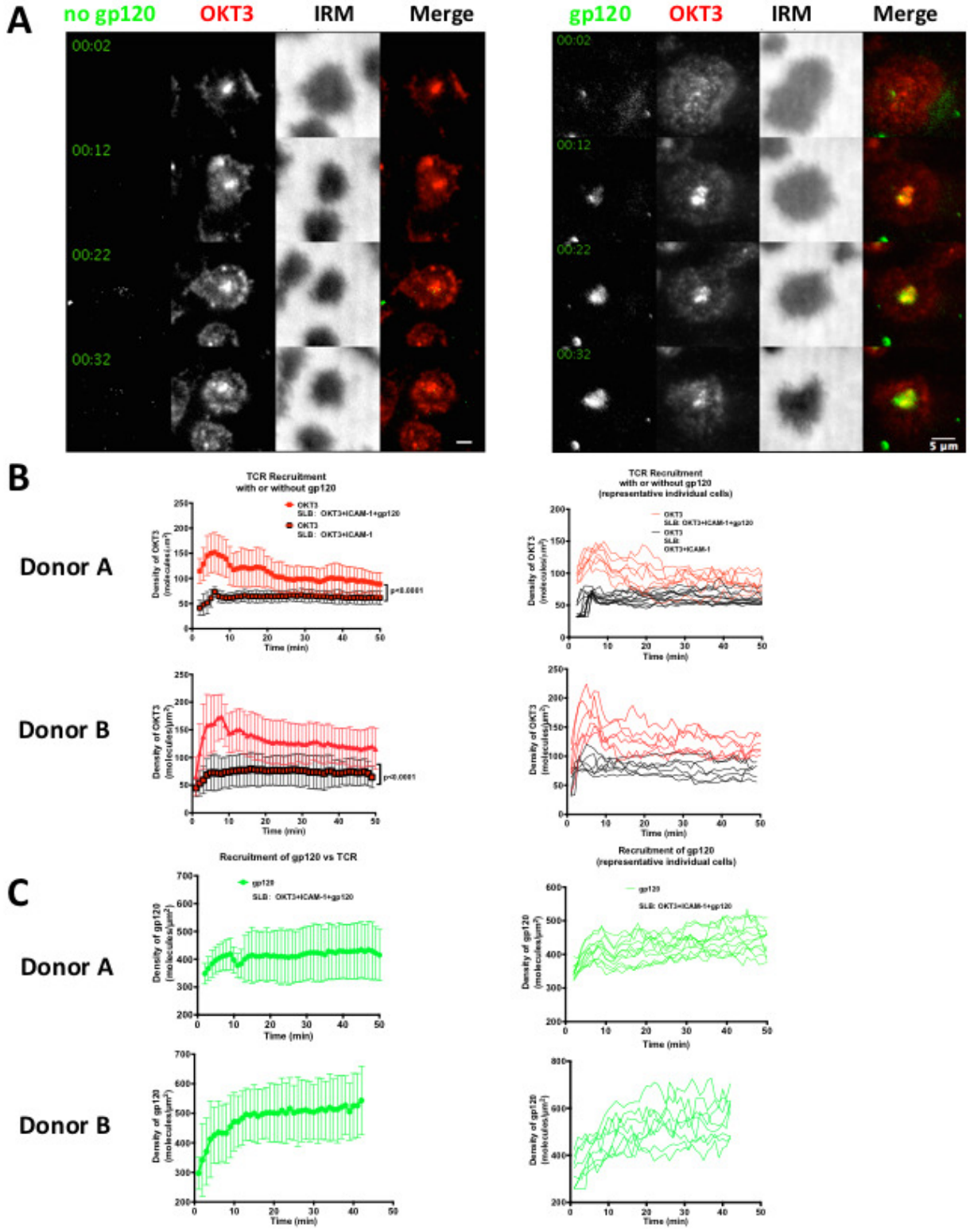

Fig. 3

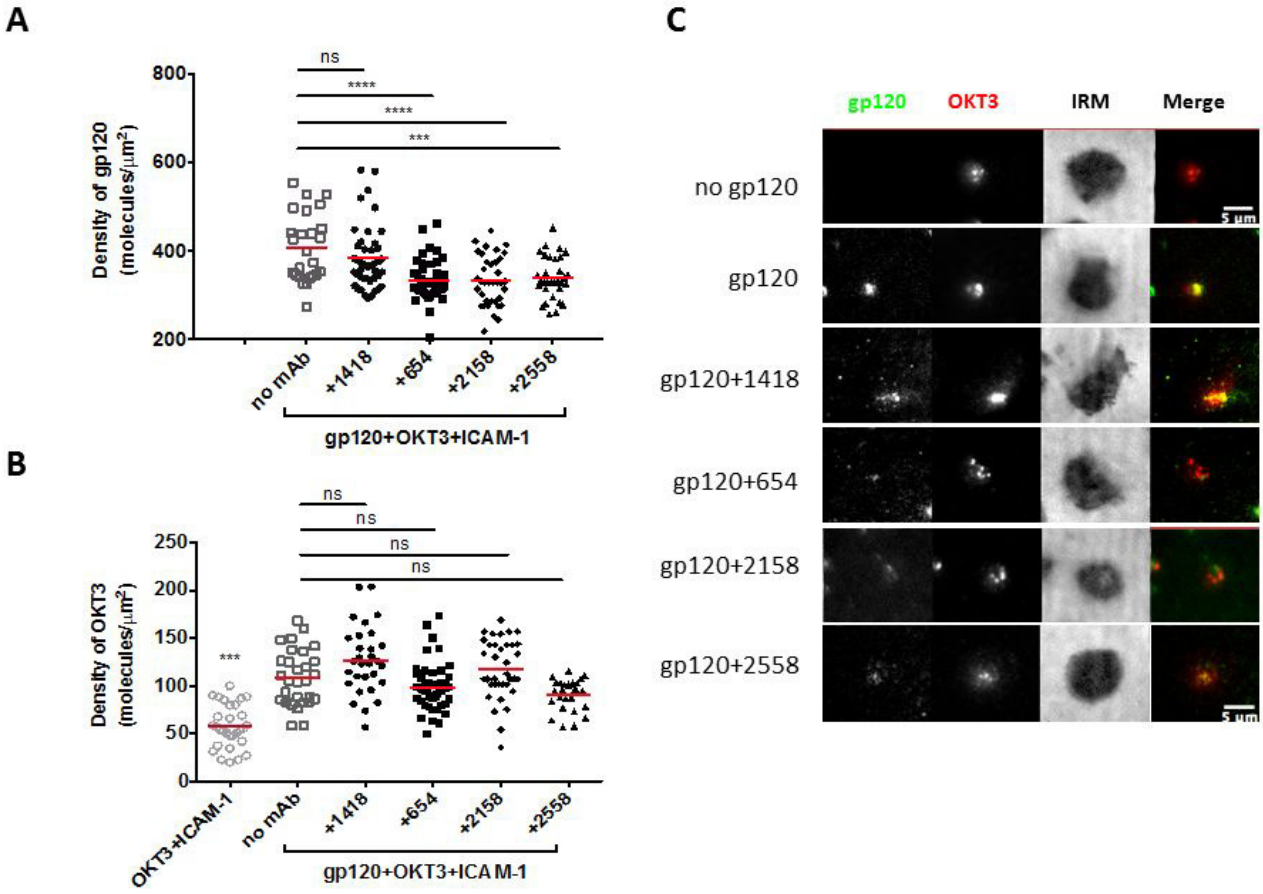

Fig. 4

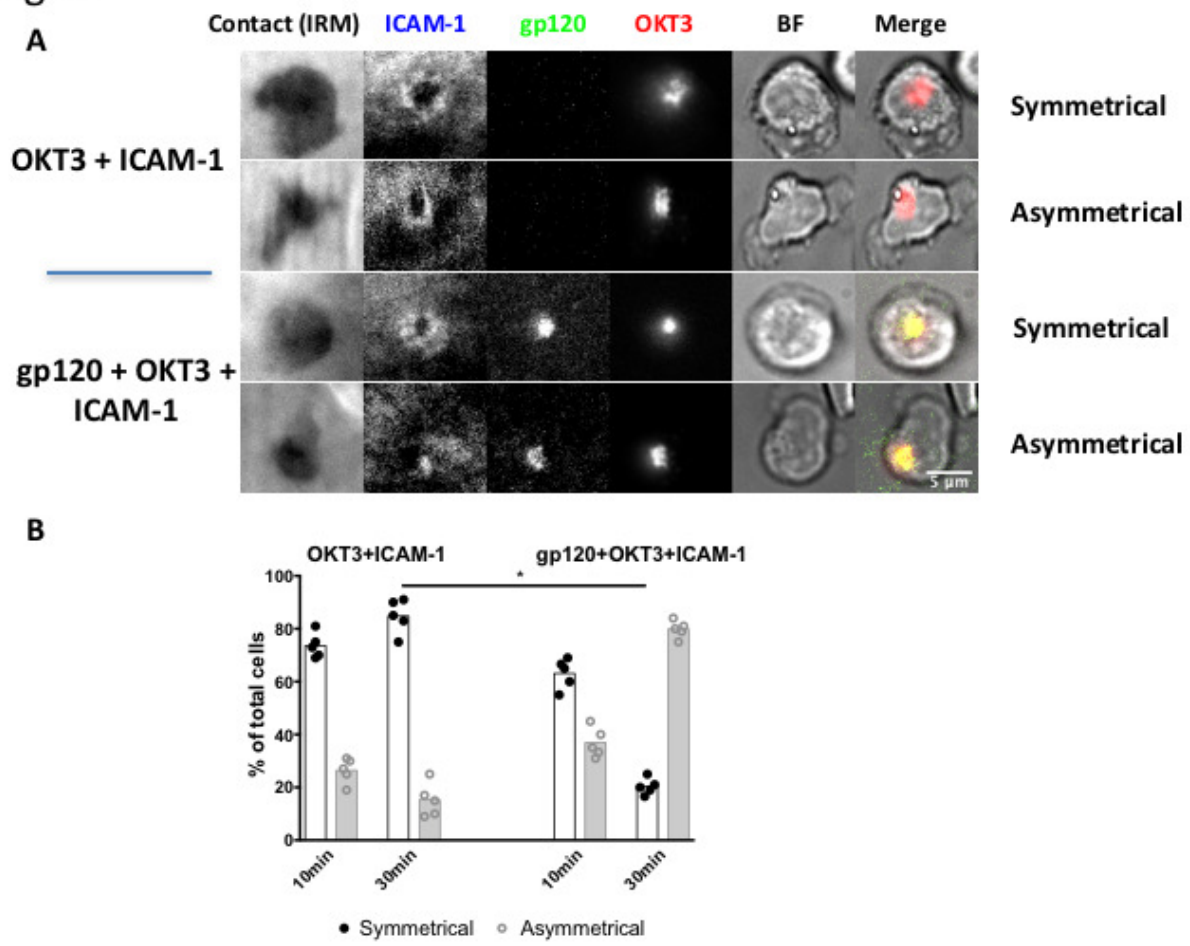

Fig. 5

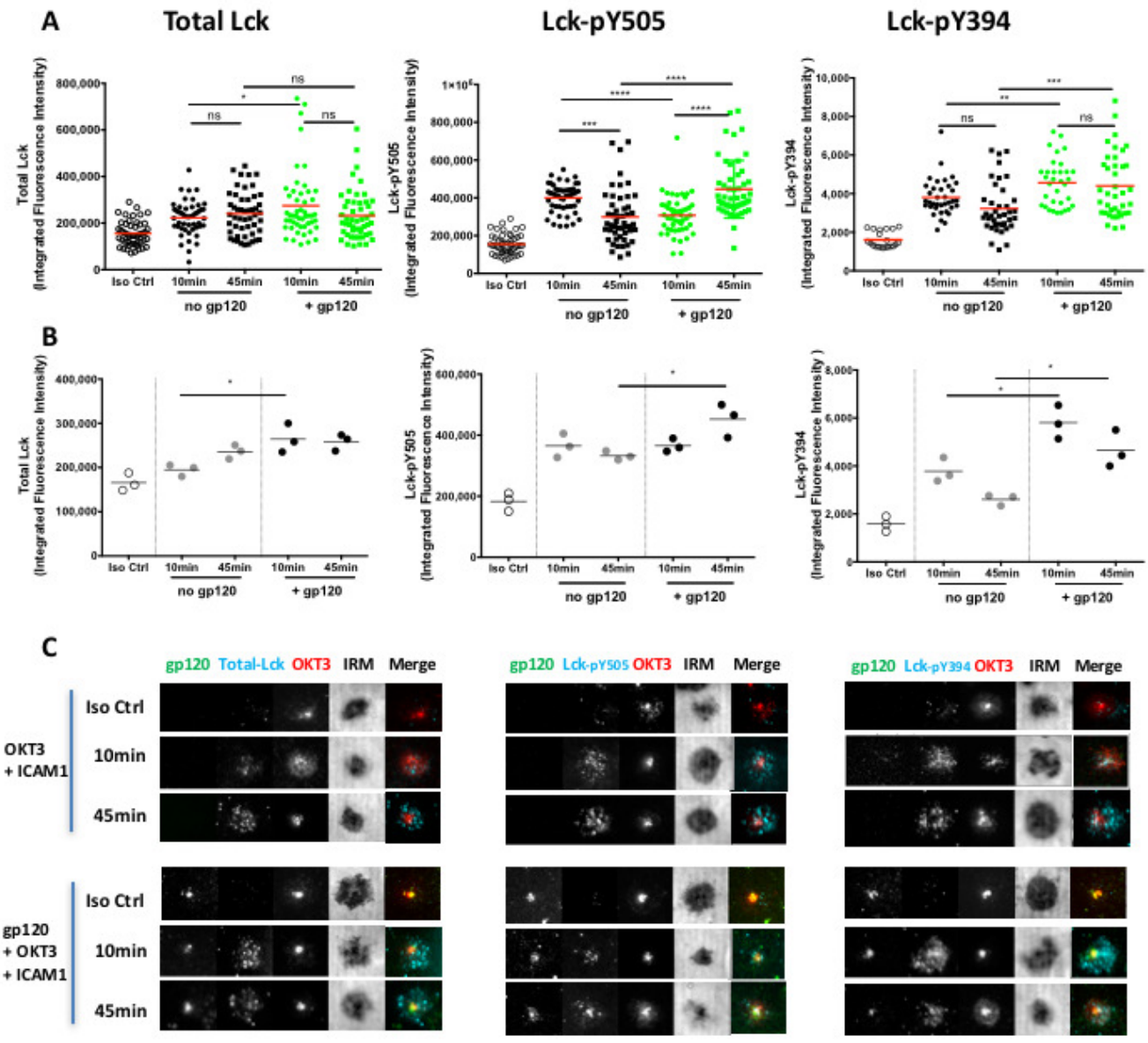

Fig. 6